NASA Technical Memorandum 105745

Results of a Low Power Ice Protection System Test and a New Method of Imaging Data Analysis

Jaiwon Shin and Thomas H. Bond
Lewis Research Center
Cleveland, Ohio

and

Geert A. Mesander
United States Air Force
Tinker Air Force Base, Oklahoma

Prepared for the
48th Annual Forum and Technology Display
sponsored by the American Helicopter Society
Washington, D.C., June 3–5, 1992

NASA

Results of a Low Power Ice Protection System Test and a New Method of Imaging Data Analysis

Jaiwon Shin and Thomas H. Bond
Aerospace Engineer
National Aeronautics and Space Administration
Lewis Research Center
Cleveland, Ohio

Geert A. Mesander
United States Air Force
Oklahoma City Air Logistics Center
Tinker Air Force Base, Oklahoma

ABSTRACT

Tests were conducted under a USAF/NASA Low Power De-icer program on a BF Goodrich De-Icing System's Pneumatic Impulse Ice Protection (PIIP) system in the NASA Lewis Icing Research Tunnel (IRT). Characterization studies were done on shed ice particle size by changing the input pressure and cycling time of the PIIP de-icer. The shed ice particle size was quantified using a newly developed image software package. The tests were conducted on a 1.83 m (6 ft) span, 0.53 m (21 in) chord NACA 0012 airfoil operated at a 4^{o} angle-of-attack. The IRT test conditions were a - 6.7 ^{o}C (20 ^{o}F) glaze ice, and a - 20 ^{o}C (- 4 ^{o}F) rime ice. The ice shedding events were recorded with a high speed video system. A detailed description of the image processing package and the results generated from this analytical tool are presented here.

INTRODUCTION

With the advent of the increased use of turbofan engines on modern aircraft, the engine core flow has decreased substantially, causing concern about the operation of engine bleed air equipment, i.e. hot bleed air anti-icing systems. The high cost, in terms of electrical power and weight, has always been an issue in restricting the application of electrically heated (thermal) anti-icers. Advances in new low power ice protection designs may provide opportunities to overcome the above limitations.

Presented at the AHS 48th Annual Forum, Washington, D.C., June 3-5, 1992.

Unlike conventional anti-icing systems, de-icing systems let ice accrete on the surface until there is enough mass to expel. Most of the new de-icing technologies rely on very rapid surface displacement, induced by a repulsive force, to crack and debond the ice. Once expelled, the shed ice particles are carried away from the surface by the airflow. If an engine inlet or upstream airframe component is to be protected with a de-icing system, the ice protection system needs to be designed so that shed ice particles are not big enough to damage the engine fan blades. Therefore, the quantification of shed ice particle size is very important for an application of de-icing systems on or in front of engine inlets because the potential for future use of these systems will be determined in part by the size, shape, and number of particles that the engine can safely ingest.

The tests of low power ice protection systems in the NASA Lewis Icing Research Tunnel (IRT) in 1990 by the United States Air Force (USAF) Oklahoma Air Logistics Center and NASA Lewis Research Center (LeRC) resulted in the development of new test methods and data acquisition systems to capture ice shedding events and quantify ice particle size.[1] The initial image processing work to quantify ice particle size was very labor intensive and provided minimal data. It became clear a more automated and extensive data characterization package was needed. The tests also identified new questions such as the effects of input power and/or pressure and the effects of very short cycling times (less than one minute) on shed ice particle size. A follow-on test of the BF Goodrich Pneumatic Impulse Ice Protection (PIIP) system was implemented to investigate input pressure and short de-icer cycling times effects on shed ice particle size. This test provided a good opportunity to examine the new image processing package developed since the 1990 USAF/NASA Low Power Ice Protection

Program IRT tests.

In this paper, the shed ice particle size results from the PIIP system test will be presented. A detailed description of the experimental method and the image processing capability will also be included.

TECHNICAL APPROACH

To eliminate any geometry sensitive issues in regard to both hardware installation and operation, a generic airfoil with a relatively mild leading edge radius was chosen. Two icing conditions were chosen: a glaze ice, and rime ice. Both reflect ice accretions that have historically been hard to remove. The key parameters focused on in this test were PIIP input pressure and cycling time. To quantify shed ice particle size, a series of baseline conditions were run and then each parameter was varied individually to gage the effects on system attributes. Shed ice information was captured during each run on high speed videography and occasionally on high speed 16 mm motion pictures. The data from the high speed videography was coupled to an image processing software package that resided on a workstation platform. This allowed the transfer of digitized visual information to a computer where the shed ice particle distributions and sizes were calculated through pixel identification and scaling techniques.

HARDWARE AND SYSTEM DESCRIPTION

Icing Research Tunnel

The NASA LeRC IRT is a closed-loop refrigerated wind tunnel. A 5000 hp fan provides airspeeds up to 134 m/sec (300 mph). The refrigeration heat exchanger can control the total temperature from - 1.1 to - 42 ^{o}C. The spray nozzles provide droplet sizes from approximately 10 to 40 μm median volume droplet diameters (MVD) with liquid water contents (LWC) ranging from 0.2 to 3.0 g/m^3. The test section of the tunnel is 1.83 m (6 ft) high and 2.74 m (9 ft) wide.

Ice Protection Technologies

The Pneumatic Impulse Ice Protection system was designed and developed by BF Goodrich[2] (Fig. 1). It uses pneumatic pressure to generate the ice debonding process. The de-icer has a matrix of spanwise tubes imbedded in a composite leading edge. The tubes lay flat in the relaxed state. When the system is activated the rapidly pressurized tubes expand slightly with a resultant distortion of the outer surface that debonds the ice (Fig. 2). The high acceleration of the skin due to the extremely fast pressure pulse launches the shattered particles into the airstream. There are a number of outer skin options: for this test it was made of polyetherether ketone (PEEK).

Model Hardware

The testing was done on a 1.83 m (6 ft) span NACA 0012 airfoil with a 0.53 m (21 in) chord (Fig. 3) and a 8.43 mm (0.332 in) leading edge radius. There was a break between the leading and trailing edges at 0.18 m (7.00 in) that allowed the front section to be removed. The leading edge was fabricated by BF Goodrich and had the ice protector integrally built into the structure. The trailing edge was made with a wood spar, foam core, and a fiberglass skin. The model was mounted vertically in the center of the test section and set at a 4^{o} angle-of-attack for the entire test.

The PIIP system was composed of spanwise tubes imbedded in a toughened polymeric core with a thin overlay sheet of PEEK. Two tubes that were located symmetrically about the leading edge were operated for ice removal in this test. The PIIP system air supply was a small compressor that provided air to a reservoir that was connected to an impulse delivery valve that released the air charge to the tubes. A micro-computer in the IRT Control Room controlled the cycling rate of the valves; the input pressure was adjusted by hand at a regulator. A back-up set of nitrogen bottles was used for supply pressure when cycling conditions were below 30 second intervals.

Kodak Ektapro 1000 Motion Analyzer

The high speed videography system was a Kodak Ektapro 1000 Motion Analyzer. It consists of an intensified imager, controller, monitor, and the Ektapro 1000 Processor. A schematic view of the system is shown in Fig. 4. The Kodak Ektapro 1000 Imager has a gated image intensifier assembly behind the lens and in front of the sensor which functions as an electronic shutter and light amplifier. This increases the imager's ability to capture events in low light and reduces the blurring of objects moving rapidly through the field of view. The Intensified Imager Controller sets the shutter and amplification functions. The gate time (the

amount of time the electronic shutter is open during each frame) can be adjusted from 10 microseconds to 5 milliseconds. The intensified imager sends its video output to the Ektapro 1000 Processor where the image data was transferred to a special cassette tape that accepts magnetic media information at up to 1000 frames per second full field of view. The Processor can play back and temporarily store the taped images, and set the communication protocols to transfer the visual information in video or digital format. Time, frame rate, session number, and other pertinent data are included in the transfer.

The Ektapro 1000 Analyzer has a resolution of 240 columns of pixels by 192 rows of pixels, and provides a video output signal compatible with either NTSC (North American) standard or PAL (European) standard video recording signal formats.

TEST METHODS

Test Conditions

Two different icing conditions were simulated: glaze and rime ice. The airspeed for the glaze ice condition was 103 m/s (230 mph) at - 6.7° C (20 °F) with 0.56 g/m^3 of LWC, and an MVD of 20 µm. The rime ice condition was at 103 m/s, - 20 °C (- 4 °F), 0.36 g/m^3, and 20 µm. Both conditions fall within calibration settings for the IRT and were chosen from the Federal Aviation Regulations (FAR 25) icing envelope for Continuous Maximum Atmospheric Icing Conditions.

The system was tested at four different input pressures: 2413, 3309, 5171, and 6895 kPa (350, 480, 750, and 1000 psi). The de-icer was fired at specified intervals during a continuous spray event. The spray time was fixed at 10 minutes, and five different cycling times were used: 5, 15, 30, 60, and 120 seconds. During the 5 second cycling interval the de-icer was only fired once per cycle. For all the remaining times, the de-icer was fired twice per cycling interval with a 3 second dwell time between pulses.

Visual Data Acquisition

A Kodak Ektapro 1000 high speed video camera system described in the Hardware section was used to collect information on ice shedding. The field of view was chosen to cover the mid-span of the airfoil where there is good cloud uniformity. Image resolution was set to define a particle as small as 3.2 mm^2 (0.005 in^2) for post-test analysis requirements. The high speed video imaging equipment has more severe limitations imposed on resolution capabilities than standard video transmission signals because of the sampling rates, shuttering, and amplification. This yields a system with lower illumination requirements and with high speed image capture abilities, but sacrifices the resolution expected in modern digital video camera systems. These constraints, along with the minimum threshold particle size criteria, forced the definition of a limited area of coverage for monitoring the ice shedding event. The resulting dimensions for the field of view were 0.33 m high (13 in) and 0.41 m (15 in) wide.

The Ektapro camera was positioned 1.64 m (64.5 in) away from the airfoil, shooting perpendicular to the airfoil chordwise axis to minimize the optical distortion due to angularity. It was decided to use a recording rate of 1000 frames per second. This provided non-blurred images that defined the ice particle edges, as well as enough images of the shed event to analyze ice particles before they leave the field of view. The trade-off with this equipment set-up was that the particles were well defined within the field of view, but the amount of information about the ice shed history was limited. Within the Ektapro's field of view, particles could be tracked for about 0.41 m (15 in.). To observe shed ice particles downstream of the Ektapro's field of view, a 16 mm high speed film camera was used.

With its greater resolution potential, the 16 mm visual data could provide a larger field of view (for the same shed ice particle size resolution bounds) than the high speed videography. This allowed the examination of particle size equilibrium versus airstream loads i.e., how far downstream from the ice shed location would large particles travel before the airloads did not induce any further break up.

Ice shedding was recorded twice during the spray and once after the spray was turned off. All high speed video information was stored in specially designed Kodak video tapes to preserve the original resolution for later data reduction.

An electronically gated video camera from Xybion Electronic Systems was mounted on the hatch above the tunnel test section and aimed downward, parallel to the pressure surface of the airfoil. A numbered grid map (0.0254 m squares) on the floor of the test section was included in the field of view so that when ice was expelled

outward from the airfoil surface the particle distance could be documented. The images from this camera provided information on how far ice particles travelled away from the airfoil as they were going downstream. This data was used to apply a scaling factor for depth of field correction of the Intensified Imager camera 2-D image plane.

A depth of field correction procedure was initiated prior to testing. A grid map was located parallel to the airfoil chordwise axis at several different distances from the airfoil. An image of the grid was recorded to provide reference lengths to generate scaling factors for field of view corrections.

The 16 mm high speed film camera was used in support of imaging documentation. The field of view included the whole airfoil chord and about 0.81 meters after the trailing edge, providing a much wider field of view than the Ektapro system. The trigger for the camera was tied to a master sequencer which started all the imaging equipment at the appropriate time. The film camera was typically run at 3000 frames per second and provided pictures with slightly higher resolution than the Ektapro pictures (due to the larger field of view that the film camera covered). Grid map pictures were also taken in the same manner as for the Ektapro system.

A 35 mm camera with a high speed motor drive was mounted above the 16 mm high speed film camera to document ice shedding. The high speed motor drive enabled the camera to take five pictures per second at 1/8000 shutter speed. This provided sharp non-blurred images of ice shedding for some runs. For post-run photographic information, a 35 mm camera was used to document residual ice shapes and any close-up information on ice formations. In addition to the visual equipment described above, a VHS video camera was mounted on the tunnel ceiling upstream of the model to record an overall view of the test for general documentation and tunnel operation monitoring purposes.

Figure 5 provides a description of how the image processing techniques have been organized to allow either high speed videography or 16 mm high speed film to be used. Both options are necessary because of different requirements imposed on the test. The sheer volume of image information collected during an ice shedding event, the fast processing capability, and the near real time data viewing of the high speed videography make it the primary imaging tool for the shed ice tests. However, there are specific cases where very short cycling time de-icer firing intervals and large image field of view exposures are needed that exceed the resolution potential of the high speed videography. The 16 mm high speed film system can overcome these limitations and thus provide good data. Since it is much more cumbersome to reduce the images from this medium, and since the final particle resolution is limited by the digitization processing equipment resolution, the 16 mm high speed film system was not used until the limitations of the high speed videography were reached.

Figure 6 shows the set up of all of the control room visual documentation equipment.

Experimental Procedure

The standard routine for each run involved starting the icing spray when the IRT was at the specified test condition. Imaging data was taken a set period of time after the cloud was turned on. At the end of the spray and before the final de-icer cycle, the tunnel speed was brought down to idle and test personnel went inside the test section to measure pre-fire ice thickness at various spanwise locations on the leading edge and the lower surface adjacent to leading edge (Fig. 7).

Thickness measurements on the lower surface (pressure side) were made at two sites: the active region which was the area directly above the de-icer tubes, and the inactive region defined as the float area adjacent to the tubes. The upper surface (suction side) was normally clear, but measurements were made there if noticeable residual ice was present.

Once these measurements were made, and any pictorial data recorded, the tunnel was brought up to operating speed for a final shed event. This shed was captured with the high speed imaging data. The tunnel was then stopped, and a final set of post-fire residual ice measurements were taken. Spanwise locations of ice, known as cap ice left along the leading edge tip, were also documented. The model was then cleaned off for the next test.

ICE PARTICLE SIZE MEASUREMENT

Ice shedding images on Ektapro tapes were analyzed to calculate the ice particle size using a program called Whipice that was developed in Spring/Summer of 1991. Whipice runs on a

Silicon Graphics (SGI) Personal IRIS workstation utilizing its superior graphical capabilities. The program communicates with the Ektapro Processor through an IEEE-488 port. Images recorded on Ektapro tapes are digitized in the Processor and transmitted to the Personal IRIS.

The Whipice program has two main working modes: 'Acquire' and 'Analyze'. In the 'Acquire' mode, a user can control the Ektapro Processor remotely and import images stored on Ektapro tapes to the IRIS's memory. The 'Analyze' mode allows the user to view the imported images on the IRIS monitor and to process the images to make various measurements including the particle size.

The Whipice program differentiates ice particles from the background image by recognizing differences in grey level intensity. Therefore, the better the grey level (tonal) contrast between the ice particles and the background, the easier the recognition task becomes. A series of steps are required to assure the necessary level of contrast.

First, the program subtracts the static background image (the final image in an ice shedding event where all the shed ice has left the field of view) from every frame in the event (Figures 8 (a) & 8 (b)). The only information now left on the frame will be the ice particles moving across the screen. At this point the particles still contain the whole grey level spectrum. This tonal shading of the particle against the background makes it difficult for the program to define their boundaries.

The second step is to eliminate the particle recognition problem by changing all the ice particles to be just one color, and the background to be another color. This is done by selecting a threshold grey level that makes any pixels above the threshold pure white and any pixels below the threshold pure black (see Fig. 8(c)). The threshold selection process is dependent on user input - the program allows the user to adjust the threshold setting by scrolling between the pre-selection image and the threshold setting image until the two appear similar enough to satisfy the user. In this selection process small changes in threshold setting result in obvious adjustments to the particle array, so defining an accurate image representation is quite straight forward.

Finally, this selected threshold value is applied to all the frames of the shedding event. After the image contrast has been set, Whipice is ready to make an ice particle size measurement by counting the number of pure white pixels.

The program calculates particle size by counting the number of pixels within the boundary (pure white area) of the ice particle 1 pixel or larger. The pixel count is converted to an area with a physical dimension by applying a scale factor. A scaling factor (detailed in Test Methods) is necessary to provide image plane depth correction because the ice particles travel outward from the airfoil as they go downstream. Both a thickness and density can be added which yield particle volume and mass. Whipice can generate tabular information for each image frame selected and choose either the complete distribution of particles and their respective sizes or just single particles.

A typical procedure for ice particle size measurement is as follows. An ice shed event is viewed to select frames of interests for measurement. The image processing threshold selection routine described in an earlier paragraph is performed. Then a corresponding overhead shot from the Xybion camera is found to determine the average linear distance of the particles from the airfoil surface. This is used to calculate a scaling factor which is applied to the pixel count representing the size of the particle. As each particle size measurement is completed in a frame, the program generates a table containing this information: including the number of particles, particle size, volume, and mass of each identified particle. Ice particle thickness information can be provided from a direct measurement in the image using the Whipice program or from an experimental measurement typed in as an input value.

RESULTS

Documentation for the icing encounter can be divided into two broad categories. The shed ice particle size is important when examining conditions that are pertinent to engine ice ingestion or mechanical damage on downstream aircraft components. The quantity and thickness of ice remaining on a surface have a direct relation to aero-performance concerns. During the tests, both categories were documented, however for the scope of this paper, only the results of shed ice particle size measurements are presented.

Shed Ice Particle Size

There are two aspects to consider in order to acquire valid information on shed ice particle size distribution. When an ice shedding occurs, a number of the ice particles do not reach their steady state size immediately. During the initial de-icing phase, ice particles keep breaking up as they are expelled from the airfoil surface. While in the airstream, the ice particles can break up even further from aerodynamic forces or by colliding with each other. This aspect dictates the amount of delay necessary before analysis of the shedding event should begin. The other important aspect is to capture enough particles to represent a true distribution of particle sizes. The small particles travel downstream faster than the larger ones, and the trade-off comes in trying to capture most of the small shed ice in the frame while still waiting long enough for the larger particles to be of stable size. This aspect suggests how far into the shedding event the analysis should continue. Since the field of view is fixed, these two requirements bound a window for analysis within an ice shedding event.

The actual measurement was made over several consecutive image frames within the window bound dictated by the above requirements. Ice particles rotate while being carried downstream. Since the program analyzes a two-dimensional image, a rotating particle will reflect a different size during different frames. Therefore, a particle size distribution obtained analyzing any one frame of data will not result in a representative distribution. The approach to cope with this limitation was to analyze several consecutive frames to obtain a particle distribution in an averaged sense. The number of frames analyzed depended on the character of each ice shedding event. Typically 5 to 7 consecutive frames were analyzed per shedding event.

The PIIP system was tested to investigate effects of input pressure and cycling time on ice particle size. The results are presented for both. The baseline input pressure was determined by BF Goodrich to be 3309 kPa (480 psi).

Effects of input pressure

During the 1990 USAF/NASA Low Power Ice Protection Systems test, limited runs were made with a few systems for the effects of input power and/or input pressure on the system performance. Typically, it was done during system check-out and calibration, and it appeared that input energy had an effect on system performance, but there was no time during these tests to quantify this issue. This present test further examined the effects of input pressure on shed ice particle size by operating at four different input pressures: 2413, 3309, 5171, and 6895 kPa (350, 480, 750 and 1000 psi), with up to five different cycling times: 5, 15, 30, 60 and 120 seconds. Table 1 provides a compilation of the imaging data points. Each condition tested was repeated. Test points at 30 and 60 second cycling times for 2413 and 6895 kPa were added during the last 3 days of IRT testing when the opportunity arose to extend the test matrix.

The results for 30 and 60 second cycling times for the glaze ice condition are presented here; these have test points over the entire input pressure range tested.

Figure 9 shows particle size distributions for four input pressures with a 30 second cycling time. The x-axis denotes the particle size in cm^2 and the y-axis the number of particles. Each plot in the figure contains the particle size distributions from all the analyzed frames for a specific shed event. The Whipice analysis process examines every particle 1 pixel or larger in the frame to give this distribution. The size of one pixel particle equals to 0.032 cm^2. All the figures show large numbers of small particles, with particle counts decreasing as the particle size becomes bigger. For the first three pressures (Figs. 9 (a), (b), and (c)), the particle size distribution is similar except at the ends. The number of the smallest particles changes from approximately 90 for 2413 kPa to approximately 140 for 3309 and 5171 kPa. The maximum particle size was larger for 3309 and 5171 kPa than for 2413 kPa. For the 6895 kPa, the number of the smallest particles increased to around 150 and the maximum particle size was smaller than for other pressures. Figure 9 (e) shows a combined plot of all the pressures with a curve that defines the outer bound of the particle distribution for each case. The particle size distributions for the three lower pressures lie nearly on top of each other, and therefore show insignificant sensitivity to pressure. But the particle size distribution for 6895 kPa shows that the highest pressure definitely produced smaller ice particles than the lower pressures.

Figure 10 shows particle size distributions for a 60 second cycling time. For this cycling time, the particle distributions show little change with input pressure. Figure 10 (e) shows distribution curves similar in shape to those in Fig. 9 (e), except that in Fig. 10 (e) the 6895

kPa curve is not so dramatically displaced to the left of the lower pressure curves as it is in Fig. 9 (e). The major difference in the experimental conditions represented by Figs. 9 and 10 is that the ice thickness at the 30 second cycling time is about half that at the 60 second cycling time. Therefore, for the thinner ice layer the highest pressure was more effective in breaking up the ice than it was for the thicker ice. Thus it is speculated that somewhere between the 30 second and 60 second ice accumulations there may have been a threshold ice thickness below which the highest pressure was dramatically more effective in reducing shed ice size.

Effects of cycling time

The performance of the ice protection system is directly related to the thickness of ice it is required to remove. One way to control the thickness of the ice on the surface is by changing the cycling interval between shedding events. During these tests, the input pressure was held constant, and the effects of cycling time on shed ice particle size were investigated for five different cycling intervals: 5, 15, 30, 60, and 120 seconds. Results are presented for glaze and rime ice with an input pressure of 3309 kPa.

Figure 11 shows plots of shed ice particle size versus the number of particles for each cycling time for the glaze ice condition. A trend is apparent that shorter cycling times result in smaller ice particles. The distributions show two distinctly different patterns. The first pattern, showing smaller particle distributions, is with 5, 15 and 30 second cycling times. The distribution profiles do not differ much with the cycling time. The second pattern, which shows much larger particle distributions than the first pattern, is with 60 and 120 second cycling times. As the cycling time increases there is a thicker ice on the de-icer which creates a larger particle distribution profile. These results suggest that ice thickness may be an important parameter in determining ice particle size. And as was suggested in the discussion of Figs. 9 and 10 above, somewhere between the 30 second and 60 second ice accumulations there may have been a threshold ice thickness below which the ice particles could be more easily broken up into smaller sizes.

Figure 12 shows the same type of results for rime ice. Although the distributions show two distinct patterns again, it appears that the threshold lies between 15 and 30 second with rime ice. This implies that ice type may also be affecting the ice particle distribution.

CONCLUDING REMARKS

The test was part of the continuing effort to characterize low power de-icers as a part of USAF/NASA Low Power Ice Protection Systems program. The BFG PIIP system performance was examined in terms of input pressure and cycling time. The test also provided the opportunity to check-out the new image processing technique: Whipice. This new capability to document the shed ice particle size distribution was tested and proved to be very efficient and powerful. The development of an automated image processing package to measure particle distribution was a significant improvement to the Low Power De-icer program. Whipice handles a large amount of data with an order-of-magnitude savings in time and labor compared to the previous technique, making parametric studies such as the current test possible.

This new imaging capability should prove especially useful to engine manufacturers, because they could use it during an engine inlet deicer test to obtain the distribution of shed ice particle sizes that the engine would have to ingest safely.

Considering the significant increase in the number of operational cycles for the very short firing intervals, there is a penalty in power consumed that is not returned in improved system performance in terms of shed ice particle size distributions.

REFERENCES

1. Bond, T.H., Shin, J., and Mesander, G., "Advanced Ice Protection Systems Test in the NASA Lewis Icing Research Tunnel," NASA TM 103757, Presented at the 47th American Helicopter Society Annual Forum and Technology Display, Phoenix, AZ, May, 1991.

2. Martin, C. and Putt, J., "An Advanced Pneumatic Impulse Ice Protection System (PIIP) for Aircraft," AIAA Paper 90-0492, Jan. 1990.

Table 1 High Speed Videography Shed Ice Imaging Data.

Cycling	2413 kPa (350 psi)				3309 kPa (480 psi)				5171 kPa (750 psi)				6895 kPa (1000 psi)			
Time	Glaze		Rime		Glaze		Rime		Glaze		Rime		Glaze		Rime	
(sec)	1st	rep	1st	rep	1st	rep	1st	rep	1st	rep	1st	rep	1st	rep	1st	rep
120					X	bad data	X	X	X	X						
60	X				X	bad data	X	X	X	bad data			X		X	
30	X				X	bad data	X	X	X	X	X	X	X		bad data	
15					X	X	X	X								
5					X	X	X	X								

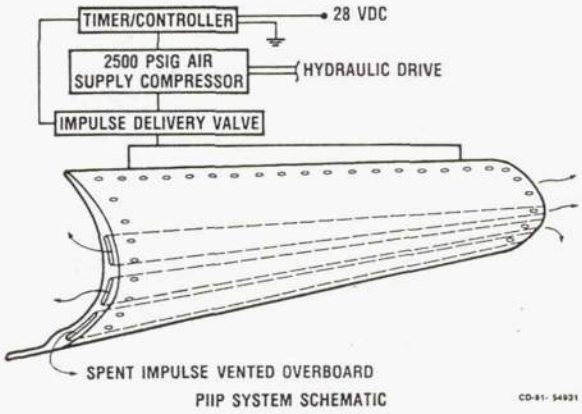

Fig. 1. BF Goodrich Pneumatic Impulse Ice Protection (PIIP) System Schematic.

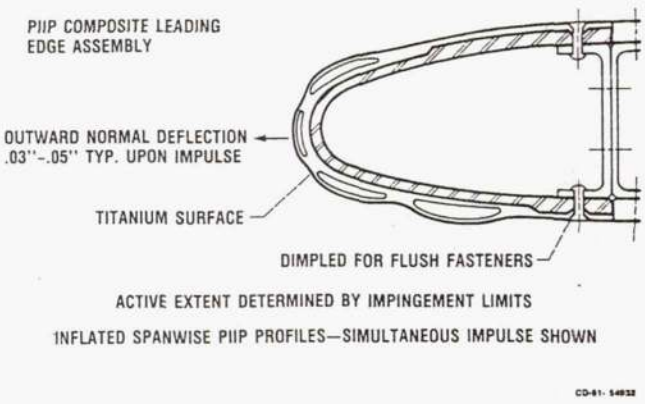

Fig. 2. BF Goodrich PIIP Composite Leading Edge Assembly (Distortion exaggerated for clarity).

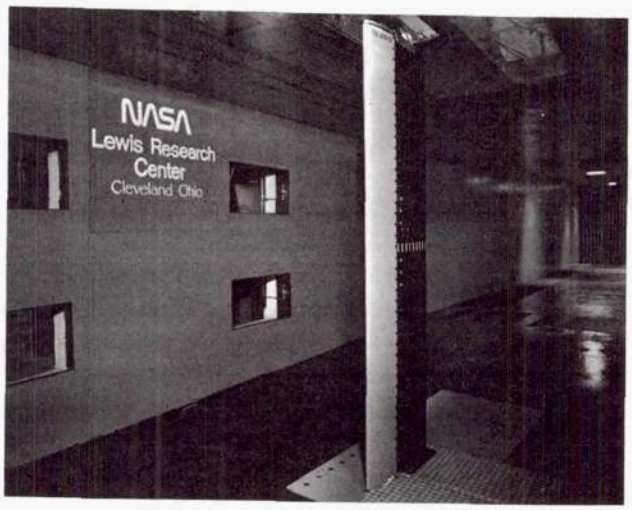

Fig. 3. NACA 0012 Airfoil with PIIP system in the IRT.

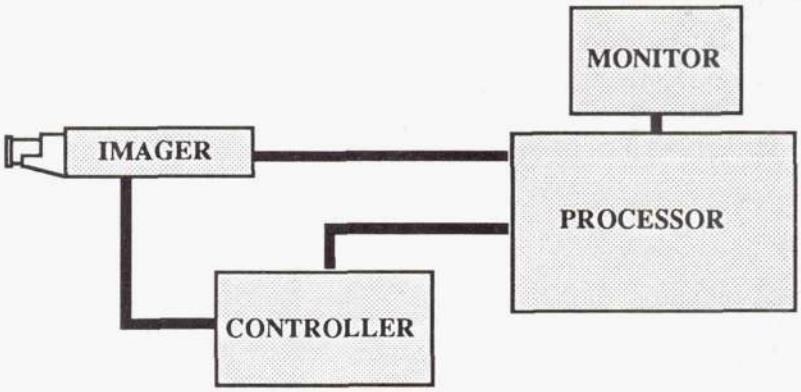

Fig. 4. Schematic View of Ektapro High Speed Videography System.

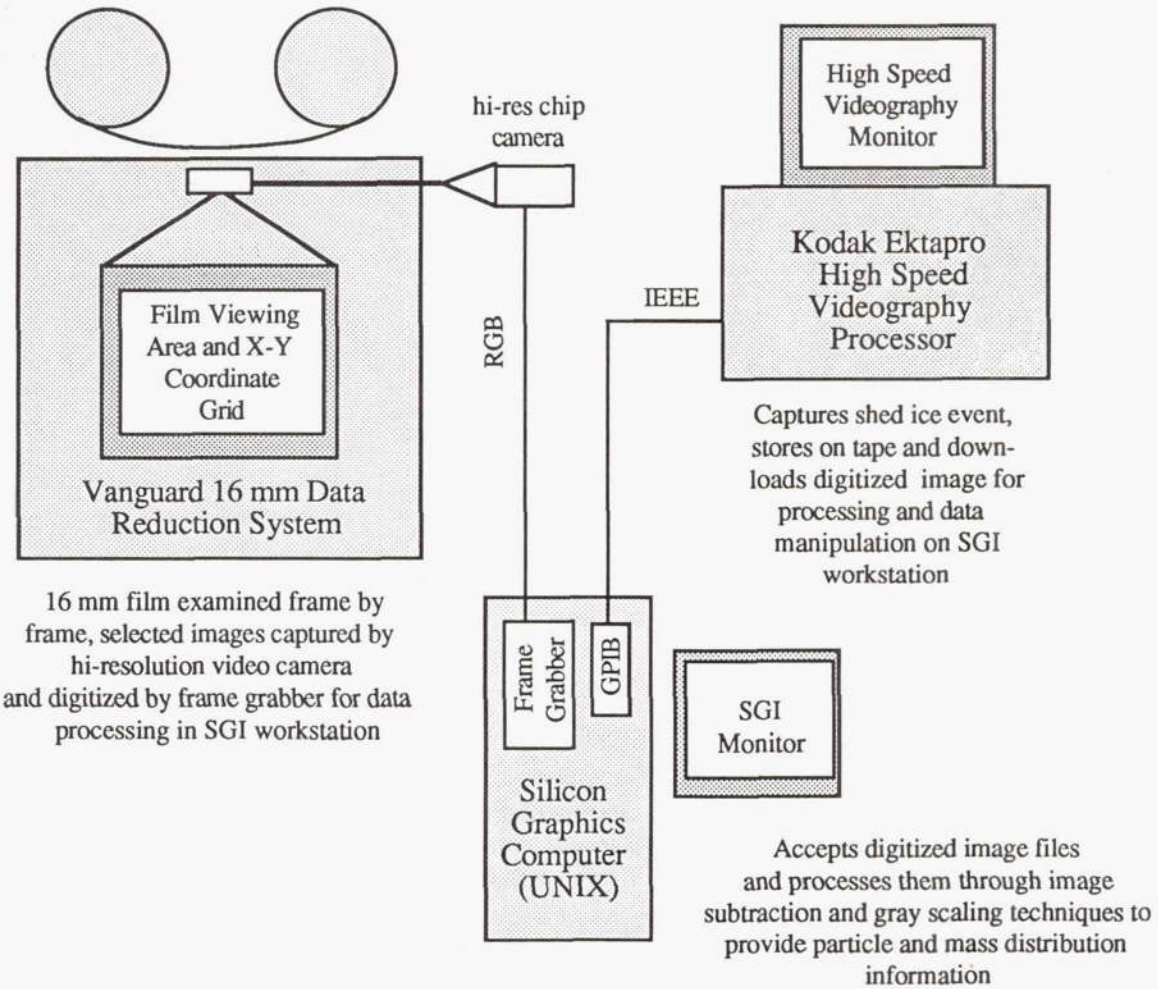

Fig. 5. De-icer Shed Ice Image Processing and Data Reduction Package.

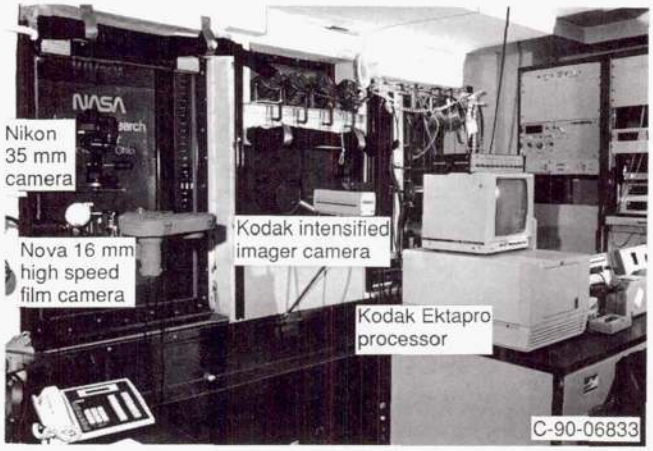

Fig. 6. Imaging Equipment in the IRT Control Room.

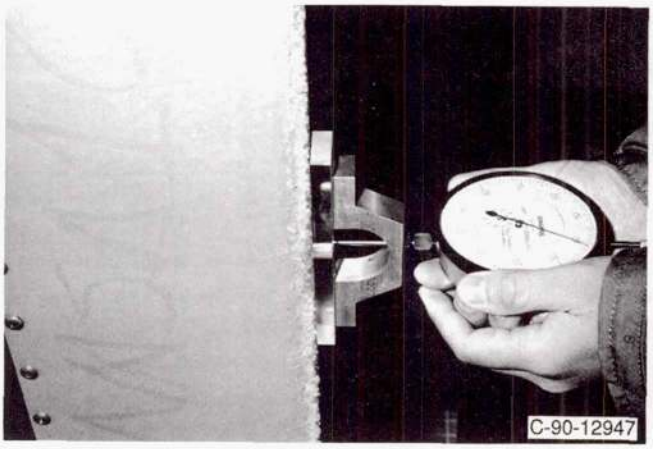

Fig. 7. Leading Edge Ice Thickness Measurement.

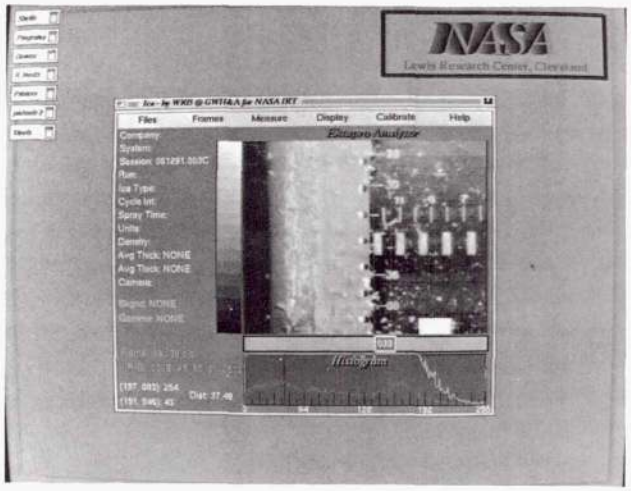

(a)

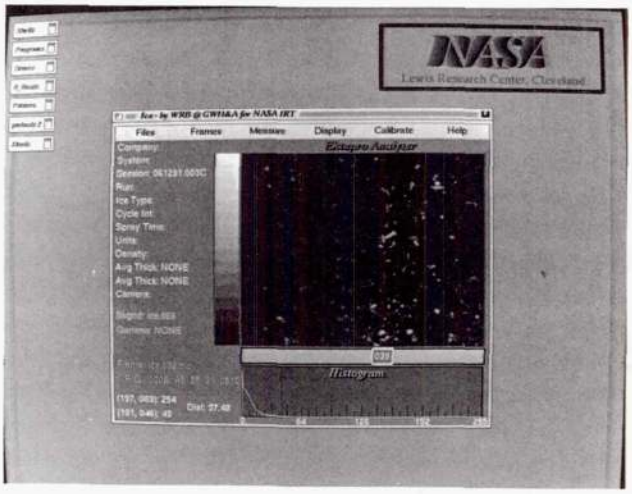

(b)

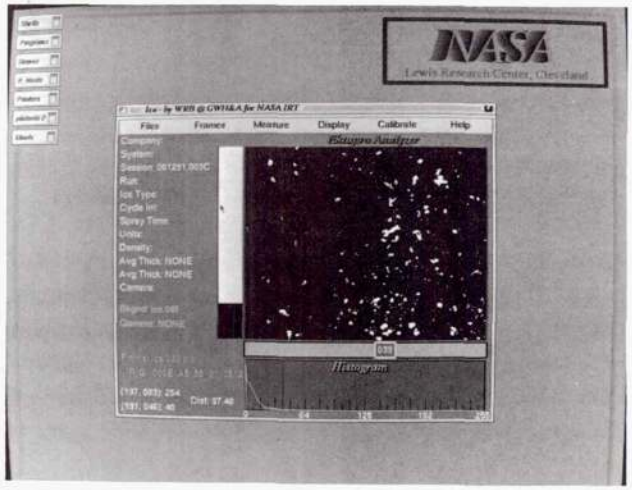

(c)

Fig. 8. Image Processing Routine for Ice Shedding Event.

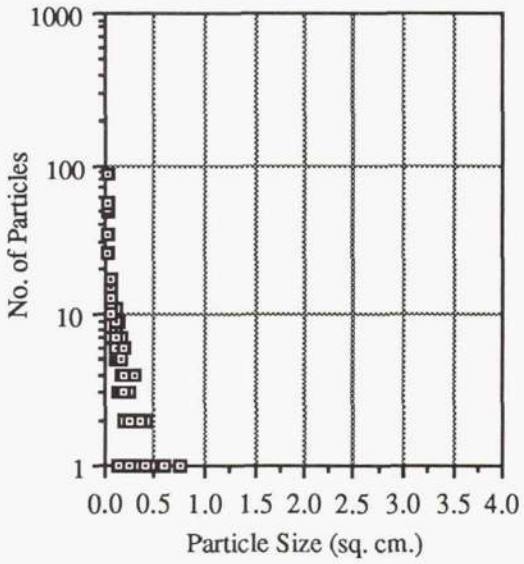

(a) 2413 kPa (350 psi)

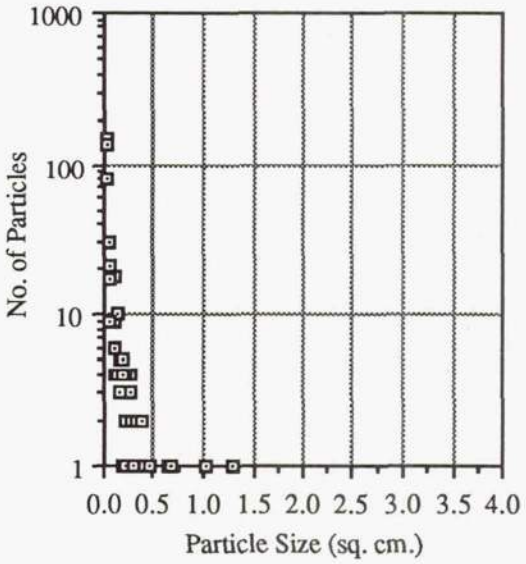

(b) 3309 kPa (480 psi)

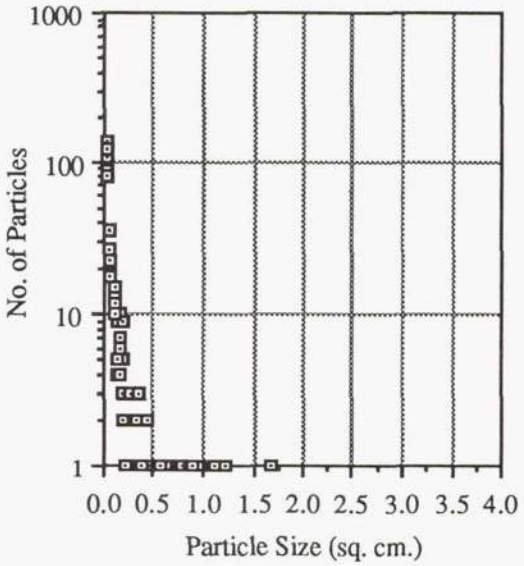

(c) 5171 kPa (750 psi)

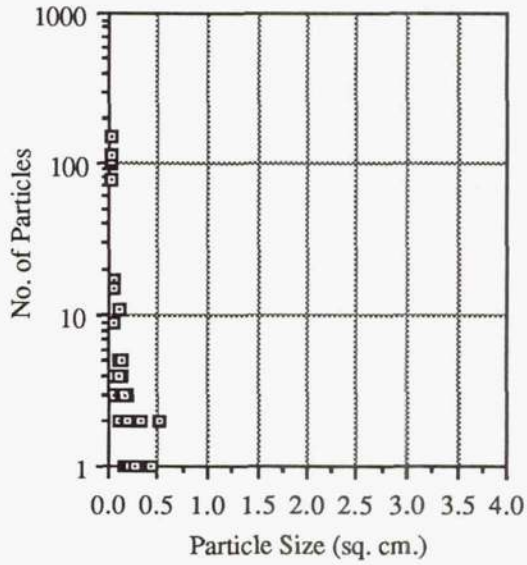

(d) 6895 kPa (1000 psi)

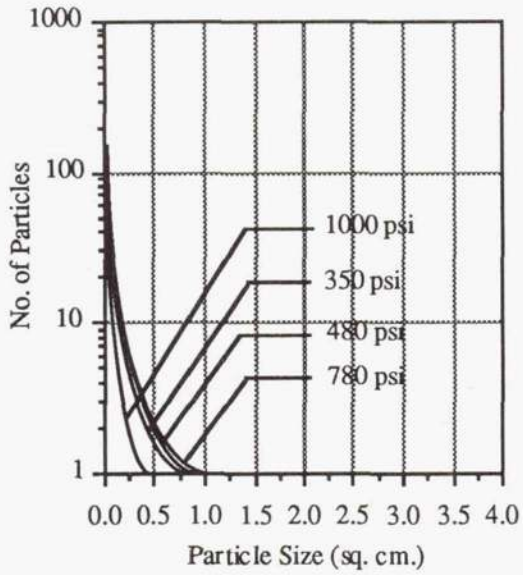

(e)

Fig. 9. Pressure Effects on Ice Particle Size Distribution with 30 sec. Cycling Interval (Glaze Ice Condition).

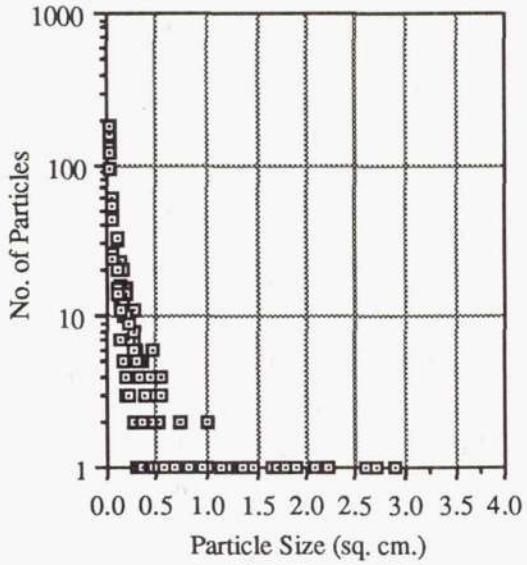

(a) 2413 kPa (350 psi)

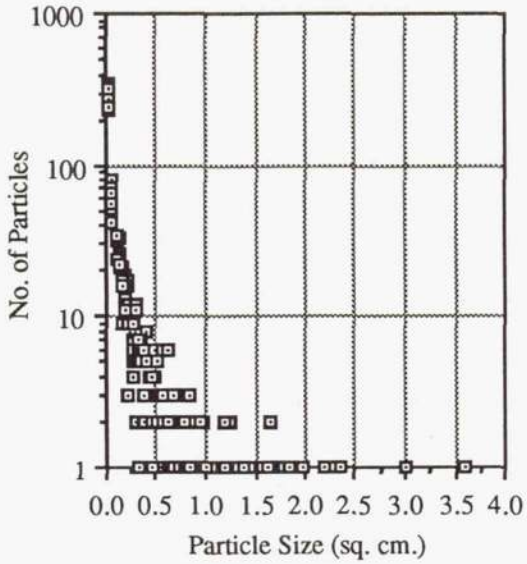

(b) 3309 kPa (480 psi)

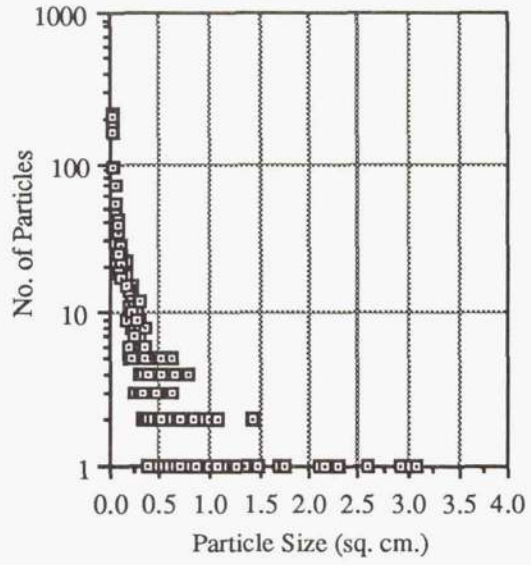

(c) 5171 kPa (750 psi)

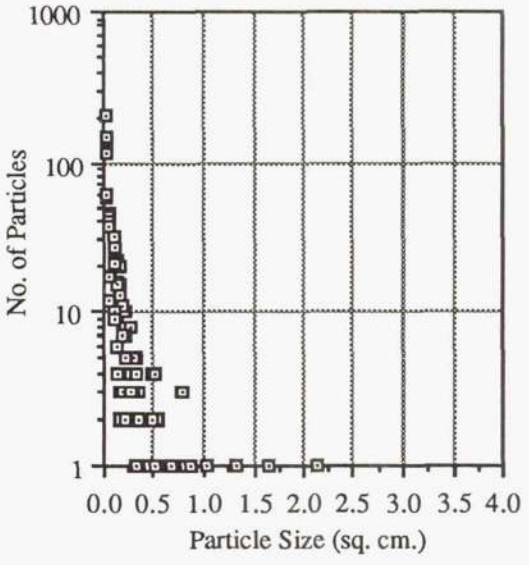

(d) 6895 kPa (1000 psi)

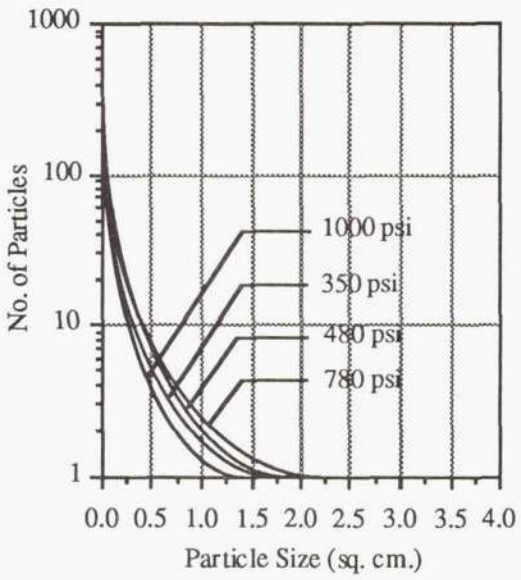

(e)

Fig. 10. Pressure Effects on Ice Particle Size Distribution with 60 sec. Cycling Interval (Glaze Ice Condition).

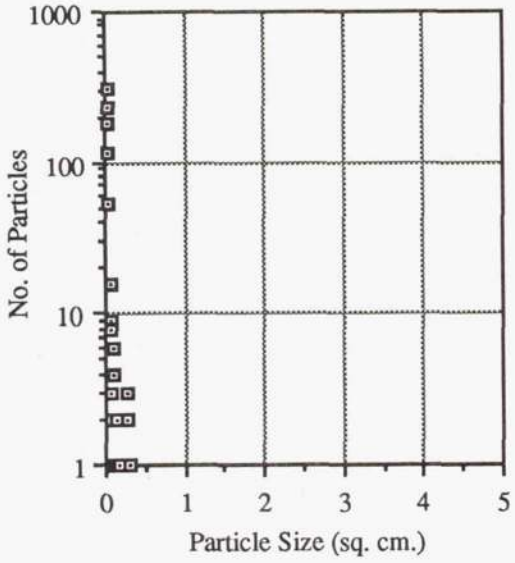

(a) 5 sec

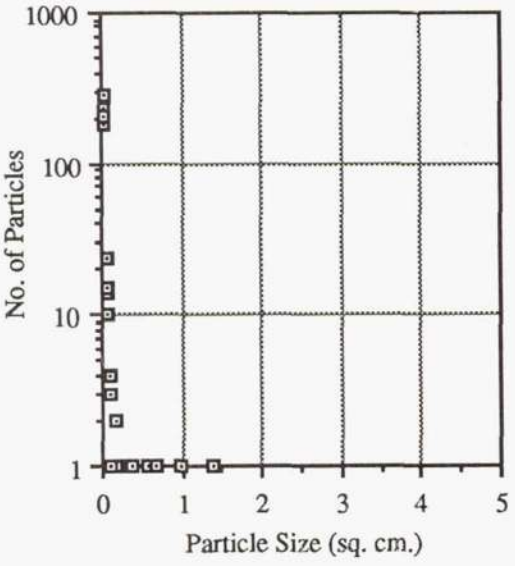

(b) 15 sec

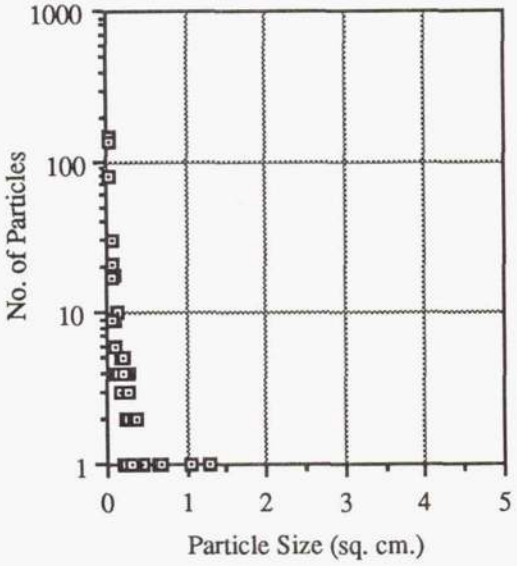

(c) 30 sec

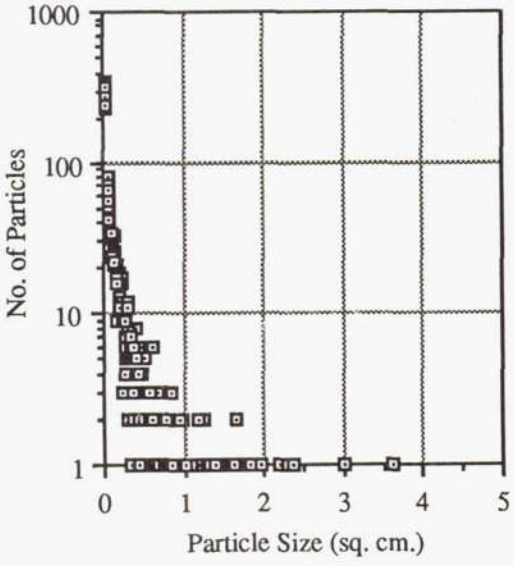

(d) 60 sec

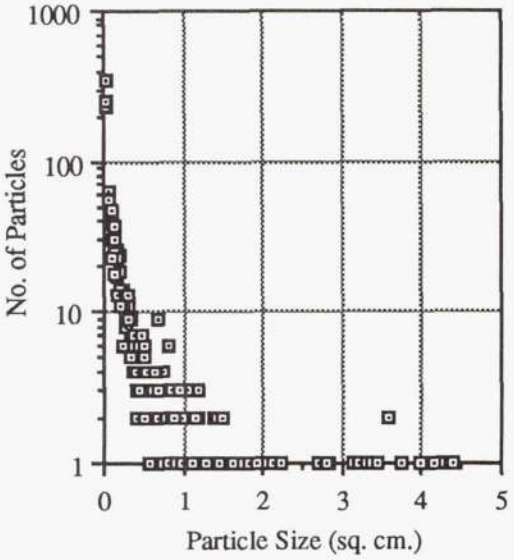

(e) 120 sec

Fig. 11. Cycling Time Effects on Ice Particle Size distribution with 480 psi (Glaze Ice Condition).

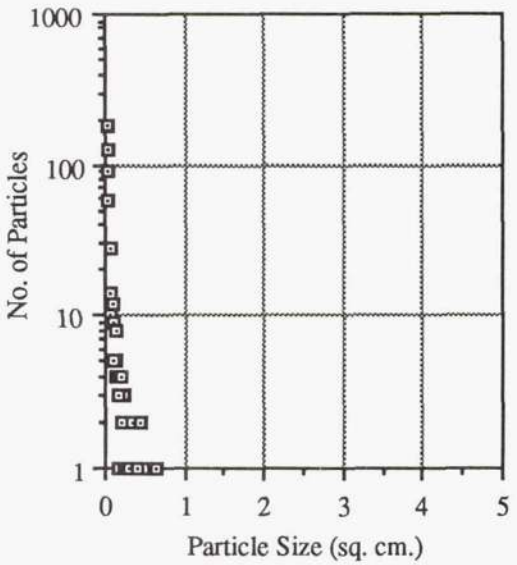

(a) 5 sec

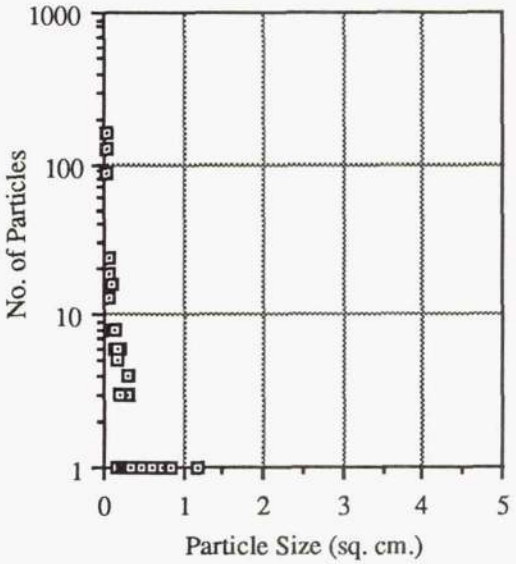

(b) 15 sec

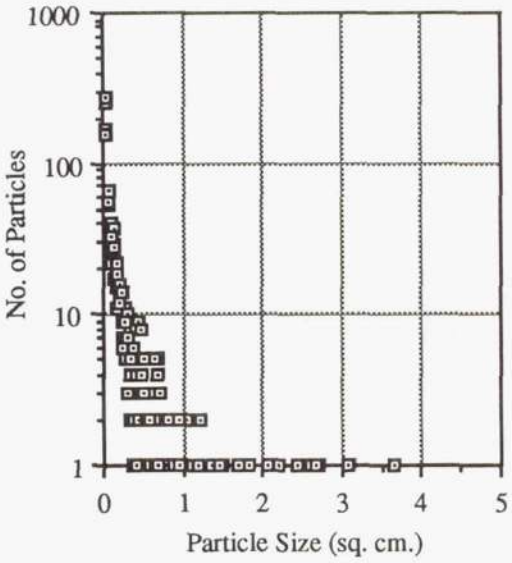

(c) 30 sec

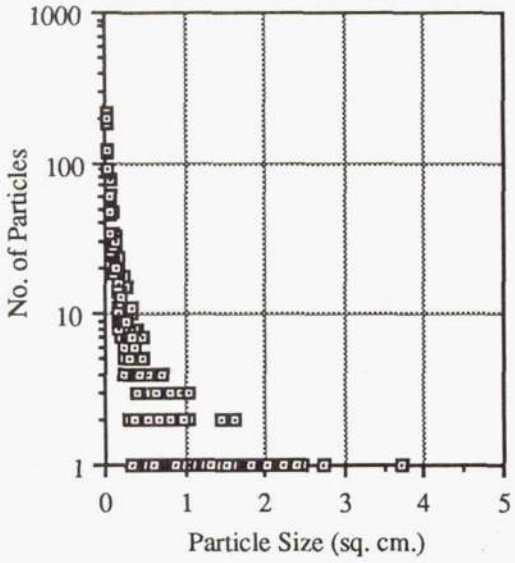

(d) 60 sec

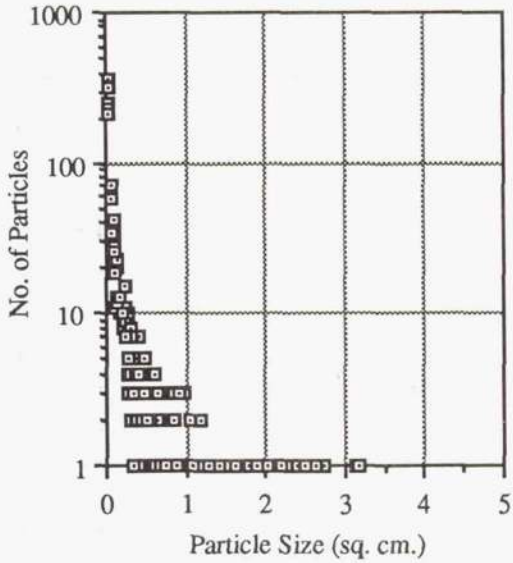

(e) 120 sec

Fig. 12. Cycling Time Effects on Ice Particle Size distribution with 480 psi (Rime Ice Condition).

REPORT DOCUMENTATION PAGE

Form Approved
OMB No. 0704-0188

1. AGENCY USE ONLY (*Leave blank*)	2. REPORT DATE	3. REPORT TYPE AND DATES COVERED
	June 1992	Technical Memorandum

4. TITLE AND SUBTITLE

Results of a Low Power Ice Protection System Test and a New Method of Imaging Data Analysis

5. FUNDING NUMBERS

WU–505–68–10

6. AUTHOR(S)

Jaiwon Shin, Thomas H. Bond, and Geert A. Mesander

7. PERFORMING ORGANIZATION NAME(S) AND ADDRESS(ES)

National Aeronautics and Space Administration
Lewis Research Center
Cleveland, Ohio 44135–3191

8. PERFORMING ORGANIZATION REPORT NUMBER

E–6930

9. SPONSORING/MONITORING AGENCY NAMES(S) AND ADDRESS(ES)

National Aeronautics and Space Administration
Washington, D.C. 20546–0001

10. SPONSORING/MONITORING AGENCY REPORT NUMBER

NASA TM–105745

11. SUPPLEMENTARY NOTES

Prepared for the 48th Annual Forum and Technology Display, sponsored by the American Helicopter Society, Washington, D.C., June 3–5, 1992. Jaiwon Shin and Thomas H. Bond, NASA Lewis Research Center; Geert A. Mesander, United States Air Force Base, Oklahoma City Air Logistics Center, Tinker Air Force Base, Oklahoma. Responsible person, Jaiwon Shin, (216) 433–8714.

12a. DISTRIBUTION/AVAILABILITY STATEMENT

Unclassified - Unlimited
Subject Category 02

12b. DISTRIBUTION CODE

13. ABSTRACT ***(Maximum 200 words)***

Tests were conducted under a USAF/NASA Low Power De-icer program on a BF Goodrich De-Icing System's Pneumatic Impulse Ice Protection (PIIP) system in the NASA Lewis Icing Research Tunnel (IRT). Characterization studies were done on shed ice particle size by changing the input pressure and cycling time of the PIIP de-icer. The shed ice particle size was quantified using a newly developed image software package. The tests were conducted on a 1.83 m (6 ft) span, 0.53 m (21 in) chord NACA 0012 airfoil operated at a 4° angle-of-attack. The IRT test conditions were a -6.7°C (20 °F) glaze ice, and a -20 °C (-4 °F) rime ice. The ice shedding events were recorded with a high speed video system. A detailed description of the image processing package and the results generated from this analytical tool are presented here.

14. SUBJECT TERMS

Low power ice protection system; Ice shedding event; Shed ice particle size; Image processing

15. NUMBER OF PAGES

18

16. PRICE CODE

A03

17. SECURITY CLASSIFICATION OF REPORT	18. SECURITY CLASSIFICATION OF THIS PAGE	19. SECURITY CLASSIFICATION OF ABSTRACT	20. LIMITATION OF ABSTRACT
Unclassified	Unclassified	Unclassified	